BIOCELL

Tech Science Press

Doi:10.32604/biocell.2025.062525 Published Online: 23 April 2025

ARTICLE

Hyperthyroidism-Induced Lymphoid Cell Activation in the Lymph Nodes and Spleen of BALB/c Mice

María Belén Rocco, Clara Requena D'Alessio, Valeria Giselle Sánchez, Horacio Eduardo Romeo[#] and María Laura Barreiro Arcos[*,#]

School of Engineering and Agrarian Sciences, Institute of Biomedical Research (BIOMED-UCA-CONICET), Pontifical Catholic University of Argentina, Av. Alicia Moreau de Justo 1600, Buenos Aires, C1107AAZ, Argentina

*Corresponding Author: María Laura Barreiro Arcos. Email: mlbarreiro@yahoo.com.ar

[#]Both authors share senior authorship of this manuscript

Received: 20 December 2024; Accepted: 27 March 2025

ABSTRACT: Introduction: Hyperthyroidism is known to affect various physiological systems, including the immune system. Thyroid hormones (THs) play a crucial role in regulating immune function, and alterations in THs levels can lead to immune dysregulation. **Objective:** Currently, we aimed to elucidate the effects of hyperthyroidism on immune function in BALB/c mice, with a focus on anatomical and histological changes in lymphoid organs, the immune response to mitogenic stimulation, mitochondrial dynamics, and reactive oxygen species (ROS) production. **Methods:** Hyperthyroidism was induced in BALB/c mice by administering thyroxine (T4; 14 mg/L) in their drinking water for 30 days. Thyroid function was assessed by measuring triiodothyronine (T3), T4, and Thyroid-Stimulating Hormone (TSH) levels. Lymphoid organ hyperplasia was evaluated through anatomical dissection. Lymphoid responses were analyzed by subcutaneous inoculation with lipopolysaccharide (LPS), followed by histological analysis of lymphoid follicles and evaluation of the morphometric parameters of lymphoid cells using flow cytometry. *In vitro* cell proliferation was quantified using the 3-(4,5-dimethylthiazol-2-yl)-2,5-diphenyltetrazolium bromide (MTT) assay. Mitochondrial morphology and density were assessed by Transmission Electron Microscopy (TEM). ROS and superoxide anion (O_2^-) production were measured using 2′,7′-dichlorodihydrofluorescein diacetate (DCFH-DA) and Nitroblue Tetrazolium (NBT) assays. **Results:** Hyperthyroid mice exhibited significantly increased T3 and T4 levels, with decreased TSH levels. Lymphoid organs, including the spleen and lymph nodes, were notably enlarged in hyperthyroid mice, with a corresponding increase in lymphoid cell number. LPS stimulation enhanced the number and size of lymphoid follicles, with hyperthyroid mice showing a greater proliferative response. TEM analysis revealed increased mitochondrial density and changes in mitochondrial structure in hyperthyroid lymphoid cells. ROS and O_2^- production were significantly higher in hyperthyroid mice, though no apoptotic activity was detected. **Conclusion:** Hyperthyroidism leads to significant alterations in immune responses, including enhanced lymphoid organ size, increased proliferation of immune cells, and elevated ROS production. These findings provide new insights into the immunomodulatory effects of thyroid dysfunction and its potential impact on immune system regulation, offering a deeper understanding of THs interactions with immune activation.

KEYWORDS: Hyperthyroidism; lymphoid organs; lymphocytic activation; mitochondria; reactive oxygen species

1 Introduction

Hyperthyroidism is a condition characterized by the overproduction of THs, primarily T3 and T4, resulting in reduced TSH levels due to negative feedback regulation. These hormones play a critical role in

metabolic regulation, cellular differentiation, proliferation, and survival, acting through both genomic mechanisms, via nuclear receptor-mediated transcription, and non-genomic pathways through their interaction with membrane receptors [1,2]. The interplay between the thyroid gland and the immune system has garnered increasing attention due to its implications in autoimmune diseases and immune modulation [3,4]. THs play a critical role in regulating both innate and adaptive immune responses [5,6]. In the innate immune system, THs enhance neutrophil activity by promoting their extravasation and stimulating respiratory burst activity. They also influence macrophage function, with T3 exhibiting pro-inflammatory effects [7,8]. Additionally, THs are essential for the proliferation and cytotoxic activity of natural killer (NK) cells and support the proliferation and maturation of dendritic cells (DCs). In the adaptive immune system, hyperthyroid states modulate the function of T and B lymphocytes through pathways involving nuclear factor kappa-light-chain-enhancer of activated B cells (NF-κB), protein kinase C, and β-adrenergic receptors [5,9]. However, despite increasing evidence of their immunomodulatory roles, the specific molecular and cellular mechanisms by which THs regulate adaptive immunity remain to be elucidated and require further investigation.

At the cellular level, hyperthyroidism induces significant metabolic changes, increasing energy demands that are met through mitochondrial oxidative phosphorylation [10]. This process not only generates ATP through oxidation-reduction reactions but also produces ROS as byproducts of the respiratory chain. The O_2^- formed during this process can convert into hydrogen peroxide, which may react with transition metals to produce highly reactive hydroxyl ions. As key energy producers, mitochondria are the primary source of ROS, contributing to the oxidative stress observed in hyperthyroid tissues [11]. Moreover, the existence of T3 receptors in mitochondria highlights their involvement in regulating mitochondrial function and cellular metabolism, reinforcing the connection between THs activity, oxidative stress, and metabolic regulation [12,13].

ROS are essential for cellular signaling, playing a key role in processes like lymphocyte proliferation and immune responses [14]. However, excessive ROS production can lead to oxidative stress, causing damage to biomolecules, cell cycle arrest, or triggering apoptosis [15,16]. The effects of ROS on cellular physiology are complex; at moderate levels, ROS support lymphocyte activation and proliferation, while at high levels, they can be cytotoxic and induce cell death [17].

The present research was designed to investigate the effects of hyperthyroidism on histological changes in lymphoid organs and immune responses during mitogenic stimulation. We specifically examined the interaction between THs and immune activation, focusing on alterations in germinal center development, mitochondrial dynamics, and ROS production. The present findings offer new insights into the immunomodulatory effects of hyperthyroidism, highlighting its role in lymphoid tissue remodeling, immune cell proliferation, and oxidative stress. These results may contribute to understanding the immune-related consequences of thyroid dysfunction and its potential impact on host defense and disease progression.

2 Materials and Methods

2.1 Animal Model

Ten-week-old female BALB/c mice were purchased at the Institute of Biomedical Research, Buenos Aires, Argentina and were housed in ventilated cages under controlled conditions, including a 12-h light/dark cycle, a temperature range of 18°C–20°C, and unrestricted access to food and water. The mice were randomly assigned to control and hyperthyroid groups following Animal Research: Reporting of *In Vivo* Experiments (ARRIVE) guidelines. The hyperthyroid group was treated with 14 mg/L of T4 (Sigma-Aldrich, T2501, St. Louis, MO, USA) dissolved in their drinking water for 30 days whereas the control group received only the

vehicle [18]. All experimental procedures were approved by the Institutional Committee for the Care and Use of Laboratory Animals at the Argentine Catholic University (CICUAL #009/2016).

2.2 Hormone Quantification

Blood samples were obtained from the retro-orbital venous plexus under anesthesia and then, the animals were euthanized. Serum was isolated by centrifugation at 1500× *g* (Denville Scientific 260D Microcentrifuge, NJ, USA) for 10 min at 4°C. The levels of T3, T4, and TSH in the serum were measured using a Electrochemiluminescence Immunoassay (ECLIA) on an automated analyzer (Cobas e411, Roche Diagnostics, Basel, Suiza), employing commercially validated diagnostic kits (Cobas e T3 II and Cobas e T4 II, Elecsys TSH, Roche Diagnostics).

2.3 Histological Analysis of Lymphoid Tissues

Animals were subcutaneously injected with 5 µg of lipopolysaccharide (LPS) from *Escherichia Coli* serotype 026:B6 (Sigma-Aldrich, L3755, lote 111K4078) per animal in two doses, administered 15 days apart. Ten days following the final injection, the animals were euthanized by cervical dislocation, and lymph nodes and spleen tissues were extracted. The collected tissues were fixed in 4% paraformaldehyde (Biopack, 9594.08, Buenos Aires, Argentina) dissolved in cold PBS for 24–48 h at room temperature in flashing shaking. After fixation, the samples were processed for paraffin embedding using a standard dehydration protocol. Thereafter, serial sections, 7 µm thick, were obtained using a rotation microtome (HistoCore MULTICUT, Leica Biosystems, Buffalo Grove, IL, USA) and mounted onto gelatinized glass slides. The slides were dewaxed using xylene, rehydrated through a series of graded ethanol solutions, and finally immersed in distilled water. The samples were stained with Harris hematoxylin solution (Biopack, 2000083200) for 10 min, rinsed with distilled water, and subsequently stained with 0.2% eosin Y solution (Sigma-Aldrich, 109844) for 3 min. After staining, the samples were briefly washed in destilled water, dehydrated, cleared in xylene, and mounted with Canada Balsan (Biopack, 1303.08) [19]. The tissue structure was visualized using a light microscope (Axiovert 100, Zeiss, Wetzlar, Germany).

2.4 Transmission Electron Microscopy (TEM)

The ultrastructural observation of lymphoid organs was performed using transmission electron microscopy (TEM). Mice were euthanized, and lymph node and spleen tissues were cut into approximately 1 mm^3 cubes to ensure uniform fixative penetration. Samples were fixed in 2.5% glutaraldehyde in 0.1 M cacodylate buffer (pH 7.4) for 24 h at 4°C, followed by post-fixation in 1% osmium tetroxide for 2 h. Subsequently, the tissues were dehydrated through a graded ethanol series (30% to 100%) and embedded in epoxy resin. Ultrathin sections (~70 nm) were obtained using an ultramicrotome equipped with glass knives, and the sections were mounted on formvar-coated copper grids. Observations were conducted using a JEOL JEM 1200EX II transmission electron microscope operating at 80 kV at the Central Electron Microscopy Service (SCME-UNLP). The images obtained were analyzed to assess lymphocyte cellularity and ultrastructural features, including mitochondrial content and morphology, following established protocols [20].

2.5 Cell Proliferation Assay

Lymphoid cells were aseptically isolated from mouse lymph nodes and spleen. The tissues were mechanically dissociated using a metal mesh to obtain a single-cell suspension [21]. Cells were resuspended in Roswell Park Memorial Institute Medium (RPMI)-1640 culture medium (GIBCO™, 31800022, Thermo Fisher Scientific, Waltham, MA, USA), supplemented with 10% fetal bovine serum (FBS; Internegocios SA, Buenos Aires, Argentina), 1% (*v*/*v*) penicillin (100 U/mL), streptomycin (100 µg/mL) solution (Sigma-Aldrich,

P0781), and 2 mM glutamine (Sigma-Aldrich, W368401). As properly tested, cells were mycoplasma-free. Cell proliferation was determined *in vitro* by the MTT assay in 96-well flat-bottom plates. Each well was seeded with 100 µL of a cell suspension (2×10^6 cells/mL). To stimulate cell proliferation, LPS from *Escherichia Coli* serotype O111:B4 (25 µg/mL; Sigma Aldrich, L4391) was added to each well. The cell cultures were subsequently incubated at 37°C in a 5% CO_2 incubator for 72 h. Following the incubation, 20 µL of MTT solution (3-(4,5-dimethylthiazol-2-yl-2,5-diphenyl tetrazolium bromide; 1 mg/mL; Sigma-Aldrich, 475989) was added to the plates, and then were incubated for an additional 2 h to facilitate the conversion of MTT to formazan. The formazan precipitate was dissolved by adding 100 µL of a 2:1 isopropanol: distilled water solution (*v*/*v*), acidified with HCl, to each well [22]. The absorbance (OD) was measured at 570 nm using a plate reader (Multiskan, Thermo Fisher Scientific).

2.6 Gene Expression Analysis of Proliferating Cell Nuclear Antigen (PCNA)

Total RNA was isolated from lymphoid tissues using TRI Reagent® (Genbiotech SRL, TR118, Buenos Aires, Argentina) and purified by phenol-chloroform extraction following standard protocols. RNA concentrations were assessed spectrophotometrically at 260 nm using a NanoDrop ND-1000 (Thermo Fisher Scientific, Loughborough, UK). cDNA was synthesized by incubating 1 µg of total RNA with 1 µM oligo$(dT)_{12\text{-}18}$ primers (Biodynamics SRL, B071-40, Buenos Aires, Argentina), 5 mM dNTP (Biodynamics SRL, U1420), and 4 U of MMLV reverse transcriptase (Biodynamics SRL, M1705) in a final volume of 20 µL at 37°C for 1 h. PCR was performed in a thermal cycler (Bio-Rad S1000 Thermal Cycler, Bio-Rad Laboratories, Boulder, CO, USA) using 5 µL of cDNA (2.5 µg), 1 µL of primer (20 µM), and 12.5 µL of GoTaq® G2 Green Master Mix (25 mM $MgCl_2$, 25 mM dNTP, and 1.5 U of Taq polymerase; Biodynamics SRL, M7822), completing a final volume of 25 µL with RNase-free water. The β_2-microglobulin gene was used as a reference gene because its expression is unaffected by THs [23]. Specific murine primers were designed by IDT Technologies (Biodynamics SRL): for PCNA, 5′-GATGTGGAGCAACTTGGAAT-3′ (forward) and 5′-AGCTCTCCACTTGCAGAAAA-3′ (reverse); for β_2-microglobulin, 5′-GCTATCCAGAAAACCCCTCAA-3′ (forward) and 5′-CATGTCTCGATCCCAGTAGACGGT-3′ (reverse). Amplification was performed with the following conditions: initial denaturation at 95°C for 5 min, 35 cycles of 95°C for 30 s, 60°C for 30 s, and 72°C for 30 s, followed by a final extension at 72°C for 5 min. The PCR products were visualized by gel electrophoresis on a 1% agarose gel stained with ethidium bromide (Invitrogen™, 15585011, Invitrogen Corporation, Carlsbad, CA, USA).

2.7 Quantification of Intracellular ROS Levels

The production of ROS was quantified using the fluorescent marker 2′,7′-dichlorodihydrofluorescein diacetate (DCFH-DA; Sigma-Aldrich, 35845) and flow cytometry analysis. Lymphoid cells from lymph nodes and spleen were resuspended in PBS at a concentration of 1×10^6 cells/mL and incubated with DCFH-DA at a final concentration of 10 µM for 30 min at 37°C, protected from light to prevent compound photodegradation. Following incubation, cells were washed with serum-free medium, and fluorescence was quantified by flow cytometry using a 488 nm excitation laser and a 530 nm emission filter (BD Accuri™, Becton Dickinson Biosciences). Data obtained were analyzed using the BD Accuri C6 software [24].

2.8 Superoxide Anion Production

The conventional microscopic nitroblue tetrazolium (NBT) assay was used to qualitatively detect the production of O_2^- [25]. Lymphoid cells from lymph nodes and spleen (1×10^6 cells) were incubated in 24-well plates with 100 µL of NBT (1 mg/mL; Sigma-Aldrich, N-6876) in RPMI-1640 culture medium for 1 h

at 37°C. Subsequently, the formazan precipitate in the cytoplasm of the cells was observed under an optical microscope (Axiovert 100, Zeiss), and images were acquired employing an AxioCam 208 camera coupled to the microscope.

2.9 Morphometric Parameters

Lymphoid cells arising from lymph nodes and spleen were resuspended in RPMI-1640 culture medium at a final concentration of 1×10^6 cells/mL. Cell size (Forward Scatter-FSC) and granularity (Side Scatter-SSC) were assessed using flow cytometry with a BD Accuri™ C6 system. Data analysis was performed using the BD Accuri™ C6 software.

2.10 Evaluation of Apoptosis by Flow Cytometry

Lymphoid cells (1×10^6) were resuspended in 0.5 mL of staining buffer (10 mM HEPES/NaOH, pH 7.5; 0.14 M NaCl; 2.5 mM $CaCl_2$) and then incubated with 5 µL of annexin V-FITC (1 mg/mL; Sigma-Aldrich, APOAF) and 10 µL of propidium iodide (PI; 1 mg/mL; Sigma-Aldrich, P4170) for 15 min at 37°C in dark conditions [26]. The relative proportion of viable, apoptotic, or necrotic cells was examined by flow cytometry (BD Accuri™ C6, BD Biosciences).

2.11 Statistical Analysis

Data were analyzed using GraphPad Prism software, version 6.0 (GraphPad Software, La Jolla, CA, USA). Statistical comparisons between the euthyroid and hyperthyroid groups were performed using an unpaired Student's *t*-test. Before analysis, the data were tested for normality using the Shapiro-Wilk test and for homoscedasticity using Levene's test. Results are presented as mean ± standard deviation (SD). Differences were considered statistically significant at a *p*-value of less than 0.05.

3 Results

3.1 Experimental Hyperthyroidism Model

Mice were treated by adding T4 (14 mg/L) to their drinking water for 30 days to induce hyperthyroidism. Thyroid function was assessed by quantifying T3, T4, and TSH levels in the animals, as shown in Table 1. T3 and T4 levels were significantly higher in the T4-treated group compared to controls, while TSH levels were markedly lower in the T4-treated group, reflecting the negative feedback effect of THs on the pituitary gland. These findings indicate clear alterations in thyroid function parameters, consistent with the expected hormonal profiles of hyperthyroidism.

Table 1: Serum thyroid hormone levels

	Euthyroid	Hyperthyroid
T3 (ng/dl)	82.17 ± 9.26	296.35 ± 29.87**
T4 (µg/dl)	4.11 ± 0.58	23.09 ± 3.93**
TSH (ng/dl)	49.3 ± 5.2	<20

Note: Serum levels of THs in control animals or treated with T4 (14 mg/L) for 30 days, measured by the ECLIA method. Results are presented as mean ± SD. **Significantly different from the control group ($p < 0.01$); $n = 10$ animals per experimental group.

3.2 Hyperthyroidism Induces Splenomegaly and Lymphadenomegaly

Mesenteric, axillary, and pelvic lymph nodes, as well as the spleen, were excised from euthyroid and hyperthyroid mice. A clear anatomical enlargement of these tissues was observed, with splenomegaly and lymphadenomegaly in the hyperthyroid group. Compared to euthyroid mice, hyperthyroid animals exhibited an increase in both the absolute weight and the relative weight to the body weight of lymph nodes and spleen. Additionally, hyperthyroid animals showed a significant increase in the total number of lymphoid cells in the lymph nodes and splenocytes in the spleen compared to the euthyroid mice (Fig. 1).

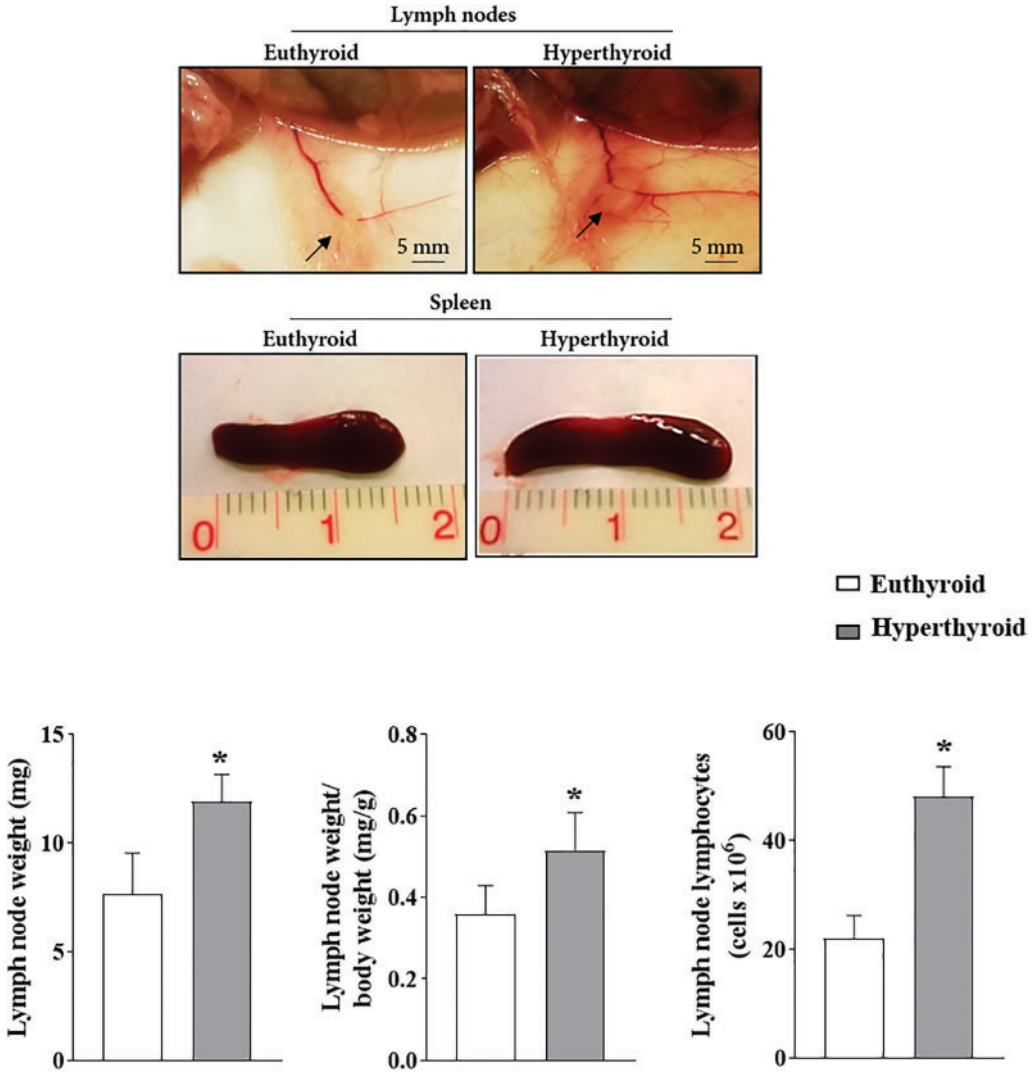

Figure 1: (Continued)

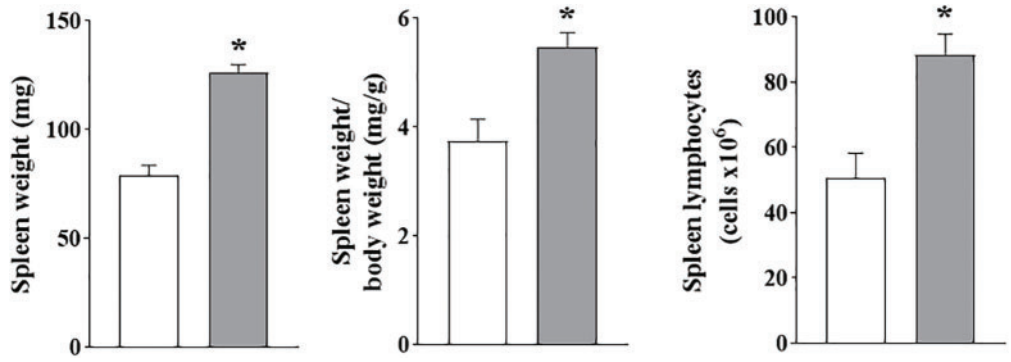

Figure 1: The impact of hyperthyroidism on lymph node and spleen size, weight, and lymphoid cell content in T4-treated animals. Mesenteric, axillary, and pelvic lymph nodes, as well as the spleen, were excised from euthyroid or hyperthyroid animals. The tissues were weighed, and the relative weight was calculated based on body weight. Lymphoid cells were counted through mechanical dissociation using a metal mesh followed by Neubauer chamber analysis. Photographs show the pelvic lymph nodes and spleen. Results are expressed as mean ± SD (n = 10 mice per group). *p < 0.05 indicates significant differences compared to the control group

3.3 Hyperthyroidism Induces Germinal Center Formation and Increases Lymphoid Cell Activation in the Lymph Nodes and Spleen of LPS-Stimulated Animals

To examine the effects of hyperthyroidism on immune responses *in vivo*, we used an antigenic stimulation protocol consisting of a primary subcutaneous inoculation with 5 μg of LPS, followed by a booster dose 15 days later. Ten days after the final inoculation, the animals were sacrificed, and histological sections of the lymph nodes and spleen were prepared to analyze the number and size of the lymphoid follicles.

In hyperthyroid mice without mitogenic stimulation, we observed an apparent increase in the number of lymphoid follicles in both lymph nodes and spleen compared to euthyroid controls. Notably, LPS stimulation significantly enhanced both the number and size of lymphoid follicles in these tissues in hyperthyroid animals (Fig. 2A), with a more pronounced response compared to euthyroid animals, indicating a heightened immune response associated with hyperthyroidism.

TEM analysis of lymphoid follicles of lymph nodes and spleens from euthyroid and hyperthyroid animals showed similar cell density in both groups. However, tissues from hyperthyroid mice exhibited reduced extracellular matrix space and a significant increase in cell size (Fig. 2B). Flow cytometry confirmed these findings, showing that lymphoid cells from the lymph nodes and spleens of hyperthyroid mice were larger and more granular than those from euthyroid ones (Fig. 2C, Table 2). No significant differences in cell size and granularity were visualized between LPS-stimulated and non-stimulated animals within each group. However, mitogenic stimulation increased the proportion of larger and more granular cells in both groups, with the effect being more pronounced in hyperthyroid animals (data not shown).

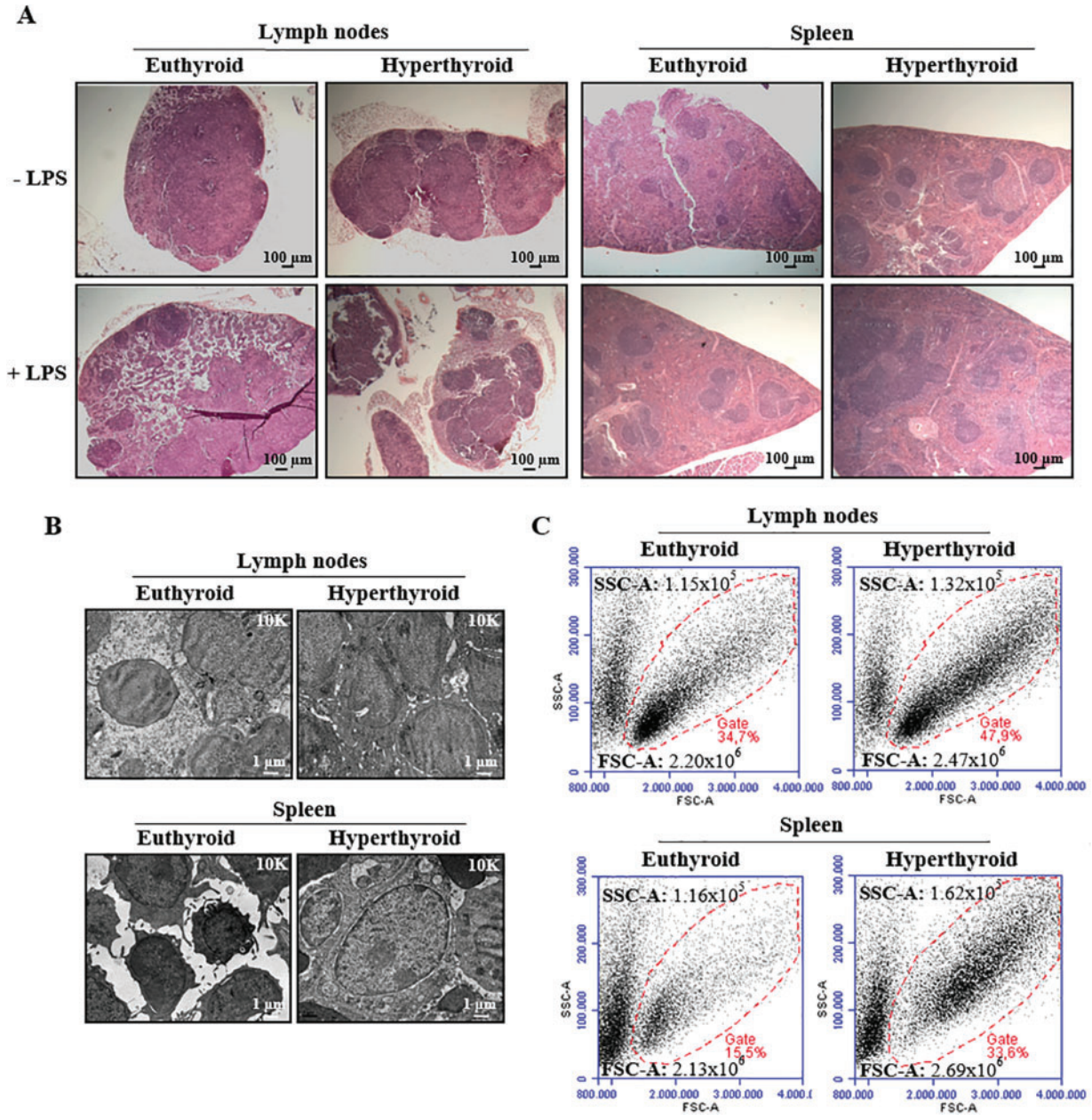

Figure 2: The effects of hyperthyroidism on germinal center formation and lymphoid cell activation in the lymph nodes and spleen of LPS-stimulated mice (A) Histological sections of lymph nodes and spleen were obtained from euthyroid and hyperthyroid animals, either unstimulated or stimulated with two doses of LPS. The animals were sacrificed 10 days after the last injection. Lymphoid tissues were stained with hematoxylin-eosin and examined under bright-field microscopy. Lymphoid follicles can be identified in the images as round areas of high cellular density with purple staining. (B) Ultrathin sections of lymph nodes and spleen from animals stimulated *in vivo* with LPS were analyzed by TEM. (C) Lymphoid cells from lymph nodes and spleen from animals stimulated *in vivo* with LPS were collected through mechanical dissociation on a metal mesh, and their morphometric parameters (granularity SSC-A and size FSC-A) were analyzed by flow cytometry. The dot plots are representative of $n = 5$ animals per experimental group

The Table 2 shows the mean ± SD values of granularity (SSC-A) and size (FSC-A) parameters of lymphoid cells from lymph nodes and spleen.

Table 2: Morphometric parameters of lymphoid cells from lymph nodes and spleen

	Lymph nodes		Spleen	
	Euthyroid	**Hyperthyroid**	**Euthyroid**	**Hyperthyroid**
Granularity (SSC-A)	$(1.18 \pm 0.12) \times 10^5$	$(1.34 \pm 0.13) \times 10^{5\star}$	$(1.14 \pm 0.12) \times 10^5$	$(1.58 \pm 0.14) \times 10^{5\star}$
Size (FSC-A)	$(2.19 \pm 0.19) \times 10^6$	$(2.53 \pm 0.21) \times 10^{6\star}$	$(2.15 \pm 0.18) \times 10^6$	$(2.64 \pm 0.22) \times 10^{6\star}$

Note: $^\star p < 0.05$ indicates significant differences compared to the euthyroid group.

3.4 Hyperthyroidism Enhances the Proliferative Response of LPS-Stimulated Lymphoid Cells from Lymph Nodes and Spleen In Vitro

To evaluate the proliferative activity of lymphocytes from the lymph nodes and spleen, we cultured lymphoid cells with or without LPS (25 μg/mL) for 72 h, corresponding to the peak of B cell clonal expansion. Proliferation was assessed by measuring metabolic activity through MTT reduction assays. Mitogenic stimulation significantly increased immunogenic responses in both lymph nodes and spleen of hyperthyroid mice compared to euthyroid controls. Although both groups exhibited enhanced proliferative responses upon LPS stimulation, the magnitude of this increase was markedly greater in hyperthyroid mice in both tissues (Fig. 3A). Additionally, LPS stimulation induced upregulation of PCNA gene expression, a marker of cell proliferation, in both lymph nodes and spleen. This upregulation was significantly more pronounced in hyperthyroid mice, indicating a heightened proliferative response (Fig. 3B).

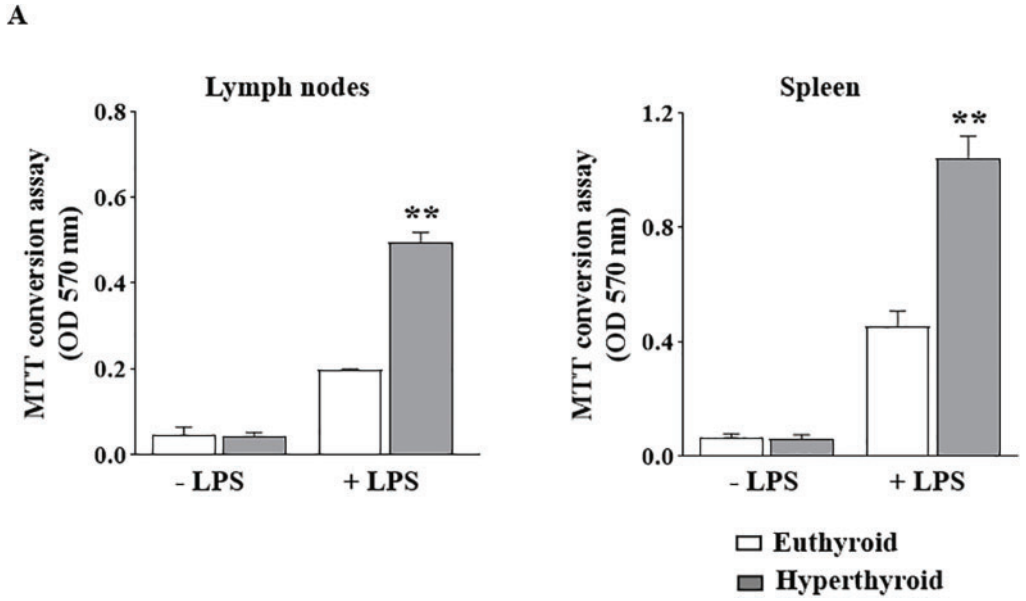

Figure 3: (Continued)

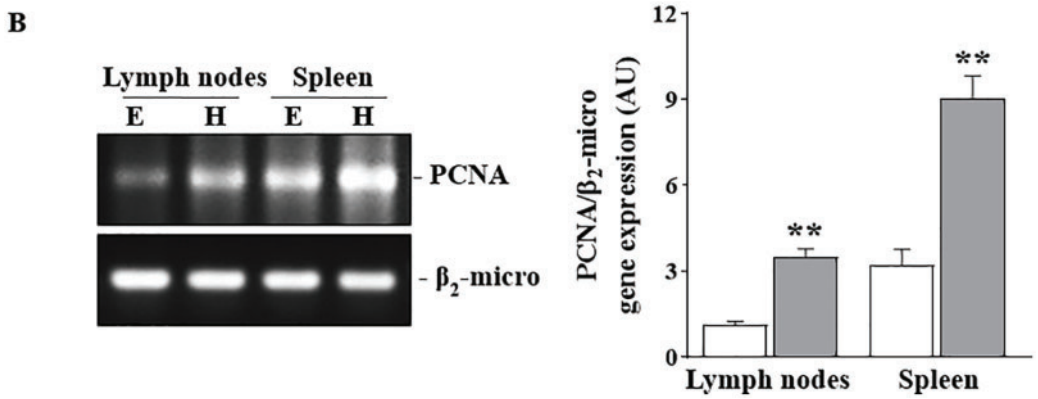

Figure 3: The impact of hyperthyroidism on the proliferative response *in vitro* of LPS-stimulated lymphocytes from the lymph node and spleen (A) Lymphoid cells from lymph nodes and spleen of euthyroid and hyperthyroid animals were cultured in 96-well plates without or with LPS (25 μg/mL) at 37°C for 72 h in a CO_2-gassed incubator. Cellular proliferation was assessed by adding MTT to the cultures, followed by quantification of absorbance at 570 nm. (B) Lymphoid cells incubated with LPS under the same conditions described in (A) were used for RNA extraction. RT-PCR was performed using specific primers for PCNA to evaluate gene expression levels. β_2-microglobulin was used as the housekeeping gene. The densitometric analysis of the amplicons is shown in the bar graph. AU represents arbitrary units. E and H represent the euthyroid and hyperthyroid groups, respectively. Results are expressed as mean ± SD (n = 5 animals per experimental group). $^{**}p < 0.01$ indicates significant differences compared to the euthyroid group

3.5 Alterations in Lymphoid Cells Induced by Hyperthyroidism

TEM analysis revealed an increase in the number of mitochondria in lymphoid cells from the lymph nodes and spleen of hyperthyroid mice compared to euthyroid controls. However, no significant changes in mitochondrial size were observed, but the variability in mitochondrial morphology was evident. In addition, mitochondria from hyperthyroid animals also exhibited increased electron density, suggesting an increase in mitochondrial cristae density (Fig. 4).

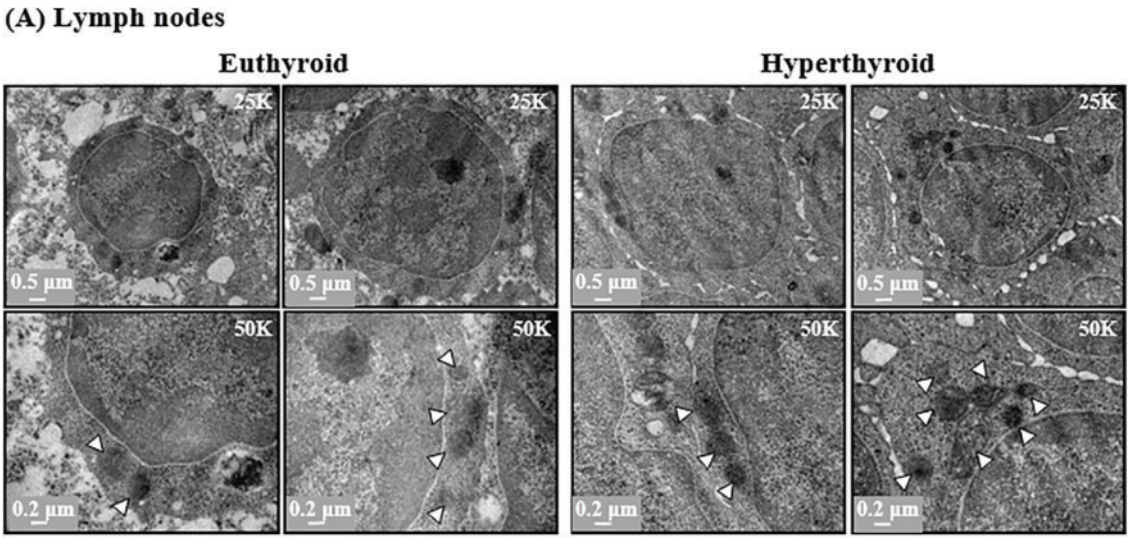

Figure 4: (Continued)

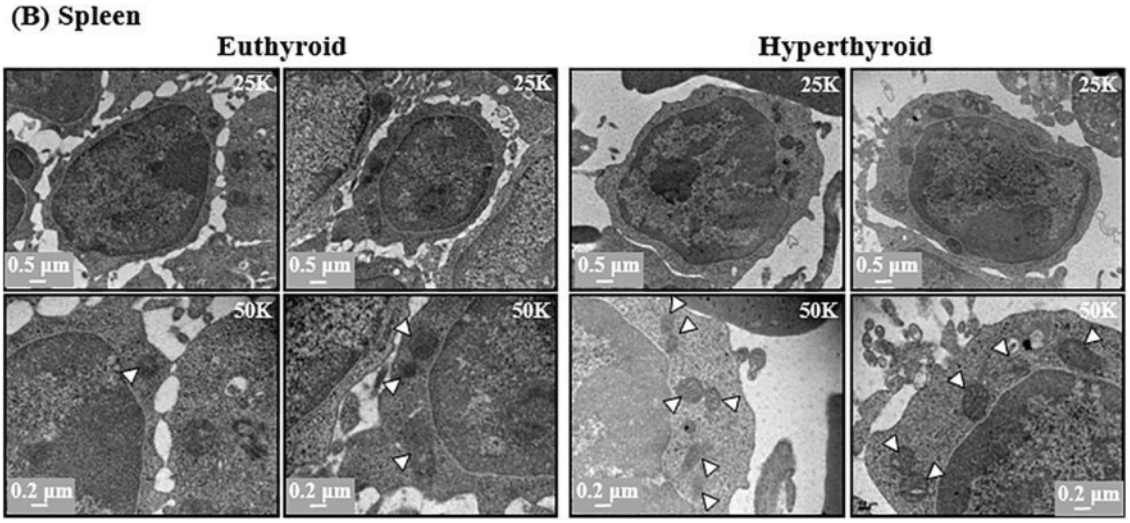

Figure 4: Effect of hyperthyroidism on mitochondrial content and morphology. The mitochondrial quantity and morphology in lymph node (A) and spleen (B) tissue from euthyroid and hyperthyroid animals were analyzed using TEM. The images are representative of lymph node and spleen sections from n = 3 animals per experimental group. Mitochondria are indicated with white arrows. Magnification 25 K (top) and 50 K (bottom). The scale bar is shown in each image

3.6 Hyperthyroidism Induces Increased ROS and O_2^- Production in Lymphoid Cells without Inducing Apoptosis

ROS production was assessed in lymphocytes from secondary lymphoid tissues of euthyroid and hyperthyroid mice using DCFH-DA staining and flow cytometry (Fig. 5A). Hyperthyroid mice showed significantly higher ROS production compared to euthyroid controls. In addition, O_2^- production was evaluated using the NBT assay and bright-field microscopy, revealing increased O_2^- levels in lymphoid cells from both lymph nodes and spleen of hyperthyroid mice (Fig. 5B). Despite the elevated ROS levels, no apoptotic mechanisms were activated, as lymphoid cells from both euthyroid and hyperthyroid mice showed similar proportions of viable cells, as well as cells in apoptosis or necrosis (Fig. 6).

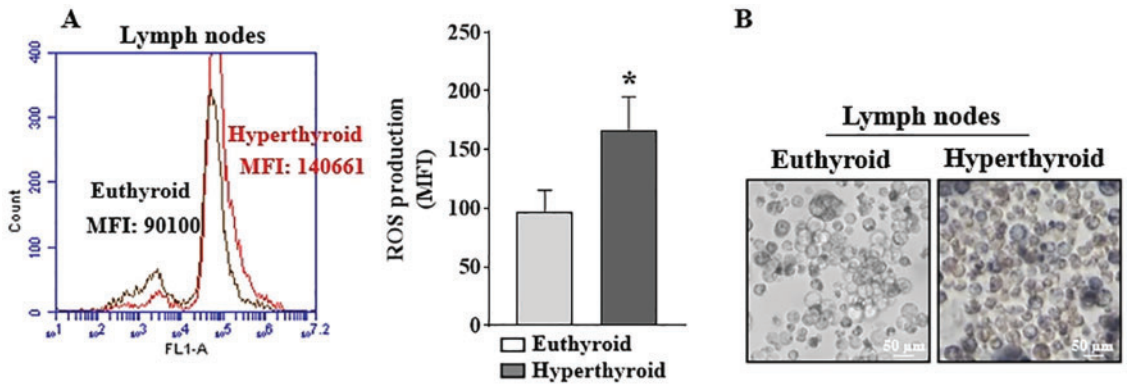

Figure 5: (Continued)

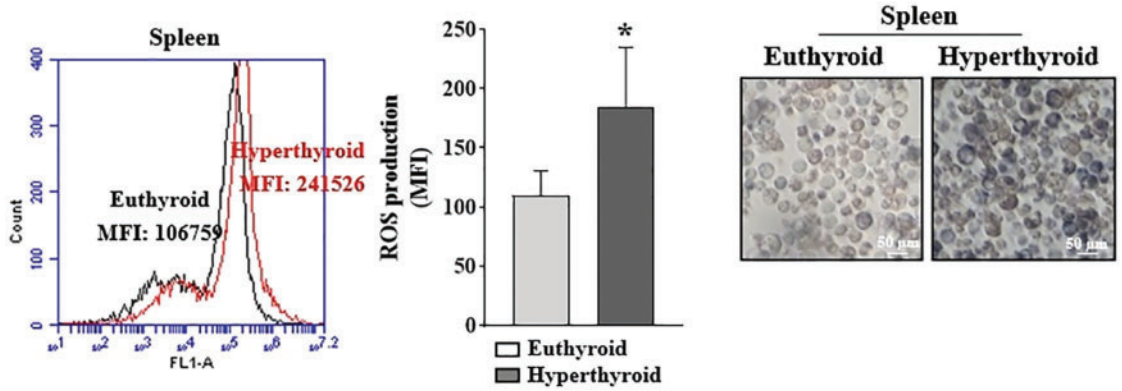

Figure 5: Effect of hyperthyroidism on ROS production. (A) The levels of ROS produced by lymphocytes from secondary lymphoid tissues of euthyroid and hyperthyroid mice were determined by incubating the cells with DCFH-DA, followed by flow cytometry. The histograms are representative of $n = 10$ independent assays and shows the mean values ± SD for each experimental group. *Significantly different from the euthyroid group ($p < 0.05$). (B) Production of O_2^- by lymphoid cells from lymph nodes and spleen of euthyroid and hyperthyroid animals was evaluated by incubating the cells in 24-well plates with NBT. The oxidized NBT product was visualized by bright-field microscopy. Representative images from $n = 6$ assays per experimental group are shown

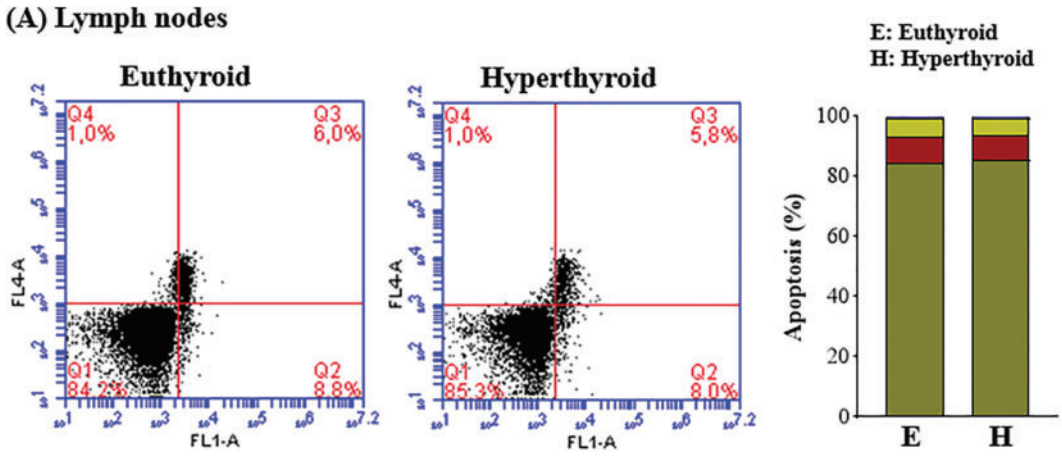

Figure 6: (Continued)

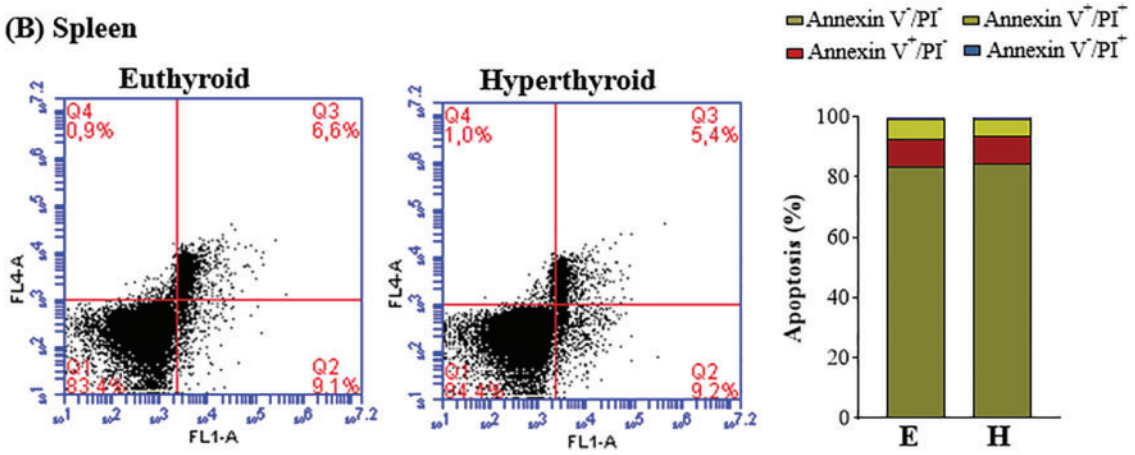

Figure 6: Effects of hyperthyroidism on lymphoid cell viability. Lymphoid cells from lymph nodes (A) and spleen (B) of euthyroid and hyperthyroid animals were stained with Annexin V-FITC and propidium iodide (PI), and apoptosis was analyzed by flow cytometry. The acquired data were processed using BD Accuri C6 software. Cells were classified as viable (Annexin V^-/PI^-), early apoptotic (Annexin V^+/PI^-), late apoptotic (Annexin V^+/PI^+), or necrotic (Annexin V^-/PI^+). No significant differences were observed between the euthyroid and hyperthyroid groups (n = 5 animals per group)

4 Discussion

Herein, we investigated the immune response and cellular alterations in hyperthyroid mice induced by T4 treatment, focusing on lymphoid tissues and the corresponding immune function. The results indicate that hyperthyroidism leads to significant changes in thyroid function, splenomegaly, lymphadenomegaly, and enhanced immune responses, as well as alterations in lymphoid cell characteristics and function.

The induction of hyperthyroidism in BALB/c mice via T4 treatment successfully altered THs levels, with significantly higher levels of T3 and T4 and a concomitant decrease in TSH, values that are consistent with the expected hormonal profile of hyperthyroidism (Table 1). Therefore, the present results validate the employment of the research model for studying the impact of hyperthyroidism on immune responses [18].

One of the most notable disclosures was the anatomical enlargement of the spleen and lymph nodes in hyperthyroid mice, which exhibited an absolute and relative weight increase when compared to euthyroid controls (Fig. 1). Additionally, the total number of lymphoid cells in these tissues was significantly greater in hyperthyroid animals (Fig. 1). The observed enlargement of lymphoid organs, suggests a state of hyperactive immune response. Further investigation into the hyperproliferative response of the germinal centers revealed that LPS stimulation increased both the number and size of lymphoid follicles in the lymph nodes and spleen of hyperthyroid mice (Fig. 2A). The enhanced follicular growth upon LPS stimulation is indicative of a heightened immune response, possibly due to the increased availability of immune cells and greater cellular activation in hyperthyroidism. Consistent with our findings, other studies have reported an increase in spleen size and cellularity, particularly in the white pulp areas, accompanied by a higher percentage of mature B cells and plasma cells, as well as an elevated frequency of pre-B and immature B cells in the bone marrow [27]. These results suggest that hyperthyroidism may promote the maturation and differentiation of B lymphocytes into antibody-producing plasma cells. Additionally, another study demonstrated changes in both cellular and humoral immunity, evidenced by an increase in thymus and spleen weight and cellularity, as well as an increase in antibody-forming cells and the relative content of T cell subpopulations [28].

Our studies were conducted in female mice, where sex hormones, particularly estrogens, may modulate the immune response [29]. Several reports indicate that variations in sex hormone levels affect the activity and lymphocytic profile of immune cells, altering cytokine production and the inflammatory response [30]. Estrogens generally have immunostimulatory effects on the adaptive immune response, while testosterone can have immunosuppressive effects [31]. Therefore, our results cannot be extrapolated to male mice, as the magnitude and type of immune response may differ due to the influence of sex hormones.

TEM analysis exhibited an increased cell size and a reduction in the extracellular matrix space in the lymphoid tissues of hyperthyroid animals (Fig. 2B), suggesting changes in tissue architecture and cellular composition [27]. Flow cytometry further confirmed that lymphoid cells from hyperthyroid mice were larger and more granular than those from euthyroid mice, which could indicate activation and differentiation of immune cells (Fig. 2C, Table 2). While LPS stimulation increased the size and granularity of lymphoid cells in both euthyroid and hyperthyroid animals, the effect was more pronounced in the hyperthyroid group, further emphasizing the enhanced immunological response under THs dysregulation.

Hyperthyroidism was associated with a significant increase in the proliferative response to LPS stimulation in lymphocytes from secondary lymphoid organs, as demonstrated by employing MTT assays and upregulation of the PCNA gene (Fig. 3). While the proliferative response was enhanced in both tissues, it was more pronounced in splenic cells compared to lymph node cells. This difference can be attributed to the distinct functions of these organs. The spleen, which filters blood and supports systemic immune responses, contains a higher number of B cells compared to lymph nodes. As a result, splenic B cells are more responsive to mitogenic signals like LPS, driving stronger activation and proliferation [32]. In contrast, lymph nodes filter lymph and detect peripheral antigens, requiring additional signals, such as those from T cells or antigen-presenting cells, to promote effective B cell proliferation in response to LPS [33]. These findings suggest that hyperthyroidism amplifies the proliferative response *in vitro* and *in vivo*, likely through enhanced B cell activation, consistent with previous studies showing that THs modulate lymphocyte activation and proliferation [34,35].

Hyperthyroidism increases lymphocytic activity in lymph nodes and spleen, which demands higher ATP production. Since mitochondria are the primary organelles responsible for ATP generation through oxidative phosphorylation in the electron transport chain, we analyzed the effects of hyperthyroidism on mitochondrial density and morphology. TEM analysis revealed an increased number of mitochondria in lymphoid cells from hyperthyroid mice, with more electron-dense mitochondria (Fig. 4), a finding consistent with enhanced mitochondrial activity [36]. While no significant changes in mitochondrial size were observed, the increased density of cristae suggests a higher content of mitochondrial proteins and enhanced energy production to meet the higher metabolic demands of activated lymphocytes [10]. This phenomenon may reflect the need for additional energy during immune activation and cellular proliferation in a hyperthyroid state. Additionally, a pronounced variability in mitochondrial morphology was observed (Fig. 4), suggesting active mitochondrial dynamics, including fusion and fission processes, which are common in cells under metabolic stress or undergoing high metabolic changes [37–39]. Mitochondrial biogenesis has been reported by other authors; however, they found that hyperthyroidism induces a disruption in the mitochondrial quality control system in liver mitochondria, leading to an increase in defective mitochondria, as was evidenced by mitochondrial swelling with a lysed matrix and reduced cristae, as well as the formation of multilamellar bodies [40]. These discrepancies with our results may reflect tissue-specific adaptations to the metabolic demands regulated by THs levels or differential tissue susceptibility to THs.

Furthermore, hyperthyroidism was found to increase ROS and O_2^- production in lymphoid cells (Fig. 5), a hallmark of oxidative stress. These findings observed in our study support previous reports linking hyperthyroidism to increased oxidative stress [41–43]. It is well established that hyperthyroid

states, characterized by increased metabolic activity, are associated with enhanced mitochondrial function [10,36,39]. During oxidative phosphorylation and ATP synthesis, mitochondrial complexes I and III generate O_2^-, which can contribute to elevated ROS levels [11]. However, beyond mitochondrial sources, other extramitochondrial enzymes, such as NADPH oxidase or xanthine oxidase, may also play a significant role in ROS production [44,45]. The activity of these enzymes could be modulated by the hyperthyroid condition, further complicating the identification of the precise sources of ROS. Therefore, a significant portion of ROS production may originate from extramitochondrial sources, which represents a limitation in our study, where we were unable to fully differentiate and quantify each source.

Despite this increase in ROS production, no apoptotic mechanisms were activated in the lymphoid cells, as both euthyroid and hyperthyroid mice exhibited similar proportions of viable cells, as well as cells in apoptosis or necrosis (Fig. 6). We have previously demonstrated in peripheral blood mononuclear cells (PBMCs) from patients with Graves' hyperthyroidism, that excess THs increase oxidative stress without compromising cell viability [46]. Additional evidence suggests that THs promote cell survival and inhibit apoptosis through multiple mechanisms, including p53 suppression, downregulation of the tumor necrosis factor-alpha/Fas cell surface death receptor (TNFα/Fas) system, decreased activation of proteolytic caspases and Bcl-2-associated X protein (BAX), and increased expression of the X-linked inhibitor of apoptosis (XIAP) [47]. The activation of the Extracellular Signal-Regulated Kinase 1 and 2 (Erk1/2) pathway has also been implicated in these protective effects [48]. Furthermore, THs not only regulate physiological processes in normal cells but also stimulate cancer cell proliferation by dysregulating key molecular and signaling pathways [49]. As we previously reported, lymphoid cells from the lymph nodes and spleen of hyperthyroid BALB/c mice upregulate antioxidant enzymes in response to THs-induced oxidative stress [43]. This suggests that the hyperthyroid state triggers a compensatory antioxidant response that mitigates oxidative damage and prevents apoptosis. Simultaneously, it may activate intracellular signaling pathways that further enhance cell survival under oxidative stress [50].

These findings indicate that while hyperthyroidism induces a heightened oxidative environment, it does not necessarily lead to apoptosis in lymphoid cells. Further research would be needed to elucidate the mechanisms regulating cell survival under these conditions.

5 Conclusion

In conclusion, our findings provide supplementary evidence that hyperthyroidism enhances immune responses, promotes lymphoid tissue enlargement, and alters cellular characteristics, including increased mitochondrial mass and ROS production. Despite these changes, hyperthyroid animals did not exhibit significant apoptotic cell death, suggesting that the increased oxidative stress did not result in overt cellular damage. Our present research highlights the complex relationship between THs and immune function, suggesting that hyperthyroidism may play a pivotal role in modulating immune responses without necessarily compromising cell viability. Regarding clinical implications, a deep understanding of the balance between immune activation and oxidative stress in hyperthyroidism could provide new insights into therapeutic strategies aimed at modulating immune responses and mitigating oxidative damage in autoimmune thyroid disorders and other oxidative stress-related conditions. Therapeutical treatments with antioxidant compounds would be a novel pathway to improve clinical outcomes. Indeed, further studies are needed to explore the underlying mechanisms that govern these effects and their implications for autoimmune disorders and other thyroid-related pathologies.

Acknowledgement: Not applicable.

Funding Statement: This work was supported by the Scientific and Technological Research Projects (PICT), grant PICT 2019-03080, funded by the National Agency for the Promotion of Scientific and Technological Research, Argentina.

Author Contributions: The authors confirm contribution to the paper as follows: Conceptualization, Horacio Eduardo Romeo and María Laura Barreiro Arcos; methodology and investigation, María Belén Rocco, Clara Requena D'Alessio, Valeria Giselle Sánchez, Horacio Eduardo Romeo and María Laura Barreiro Arcos; formal analysis, María Belén Rocco, Clara Requena D'Alessio, Horacio Eduardo Romeo and María Laura Barreiro Arcos; writing—review and editing, Horacio Eduardo Romeo and María Laura Barreiro Arcos; funding acquisition, Horacio Romeo. All authors reviewed the results and approved the final version of the manuscript.

Availability of Data and Materials: The datasets used and/or analyzed during the current study are available from the corresponding author upon reasonable request. All relevant materials are included in the manuscript or can be accessed through the provided references.

Ethics Approval: All experimental procedures were approved by the Institutional Committee for the Care and Use of Laboratory Animals at the Argentine Catholic University (CICUAL #009/2016).

Conflicts of Interest: The authors declare no conflicts of interest to report regarding the present study.

References

1. Aranda A. Thyroid hormone action by genomic and nongenomic molecular mechanisms. Methods Mol Biol. 2025;2876:17–34. doi:10.1007/978-1-0716-4252-8.
2. Contreras-Jurado SC. Thyroid hormones and co-workers: an overview. Methods Mol Biol. 2025;2876:3–16. doi:10.1007/978-1-0716-4252-8.
3. Kravchenko V, Zakharchenko T. Thyroid hormones and minerals in immunocorrection of disorders in autoimmune thyroid diseases. Front Endocrinol. 2023;14:1225494. doi:10.3389/fendo.2023.1225494.
4. Lane LC, Cheetham TD, Razvi S, Allinson K, Pearce SHS. Expansion of the immature B lymphocyte compartment in Graves' disease. Eur J Endocrinol. 2023;189(2):208–16. doi:10.1093/ejendo/lvad107.
5. Wenzek C, Boelen A, Westendorf AM, Engel DR, Moeller LC, Führer D. The interplay of thyroid hormones and the immune system-where we stand and why we need to know about it. Eur J Endocrinol. 2022;186(5):R65–77. doi:10.1530/EJE-21-1171.
6. Milling S. Beyond cytokines: influences of the endocrine system on human immune homeostasis. Immunology. 2021;163(2):113–4. doi:10.1111/imm.13347.
7. van der Spek AH, Fliers E, Boelen A. Thyroid hormone and deiodination in innate immune cells. Endocrinology. 2021;162(1):bqaa200. doi:10.1210/endocr/bqaa200.
8. Yang L, Fu MF, Wang HY, Sun H. Research advancements in the interplay between T3 and macrophages. Curr Med Sci. 2024;44(5):883–9. doi:10.1007/s11596-024-2935-6.
9. Han Z, Chen L, Peng H, Zheng H, Lin Y, Peng F, et al. The role of thyroid hormone in the renal immune microenvironment. Int Immunopharmacol. 2023;119:110172. doi:10.1016/j.intimp.2023.110172.
10. Fernández-Vizarra E, Enriquez JA, Pérez-Martos A, Montoya J, Fernández-Silva P. Mitochondrial gene expression is regulated at multiple levels and differentially in the heart and liver by thyroid hormones. Curr Genet. 2008;54(1):13–22. doi:10.1007/s00294-008-0194-x.
11. Venediktova NI, Mashchenko OV, Talanov EY, Belosludtseva NV, Mironova GD. Energy metabolism and oxidative status of rat liver mitochondria in conditions of experimentally induced hyperthyroidism. Mitochondrion. 2020;52:190–6. doi:10.1016/j.mito.2020.04.005.
12. Cioffi F, Giacco A, Goglia F, Silvestri E. Bioenergetic aspects of mitochondrial actions of thyroid hormones. Cells. 2022;11(6):997. doi:10.3390/cells11060997.
13. Sagliocchi S, Restolfer F, Cossidente A, Dentice M. The key roles of thyroid hormone in mitochondrial regulation, at interface of human health and disease. J Basic Clin Physiol Pharmacol. 2024;35(4–5):231–40. doi:10.1515/jbcpp-2024-0108.

14. Mukherjee A, Ghosh KK, Chakrabortty S, Gulyás B, Padmanabhan P, Ball WB. Mitochondrial reactive oxygen species in infection and immunity. Biomolecules. 2024;14(6):670. doi:10.3390/biom14060670.
15. Nakamura H, Takada K. Reactive oxygen species in cancer: current findings and future directions. Cancer Sci. 2021;112(10):3945–52. doi:10.1111/cas.15068.
16. Cao J, Li S, Zhang T, Liu J, Hou W, Wang A, et al. Valtrate exerts anticancer effects on gastric cancer AGS cells by regulating reactive oxygen species-mediated signaling pathways. BIOCELL. 2024;48(2):313–25. doi:10.32604/biocell.2023.043474.
17. Redza-Dutordoir M, Averill-Bates DA. Activation of apoptosis signalling pathways by reactive oxygen species. Biochim Biophys Acta. 2016;1863(12):2977–92. doi:10.1016/j.bbamcr.2016.09.012.
18. Saiz-Ladera C. Generation of a mouse model for the study of thyroid hormones regulatory effect on the immune system. Methods Mol Biol. 2025;2876:61–75. doi:10.1007/978-1-0716-4252-8_4.
19. Cardiff RD, Miller CH, Munn RJ. Manual hematoxylin and *eos* in staining of mouse tissue sections. Cold Spring Harb Protoc. 2014;2014(6):655–8. doi:10.1101/pdb.prot073411.
20. Tizro P, Choi C, Khanlou N. Sample preparation for transmission electron microscopy. Methods Mol Biol. 2019;1897:417–24. doi:10.1007/978-1-4939-8935-5_33.
21. Manhas KR, Blattman JN. Flow cytometry analysis of immune cell responses. Methods Mol Biol. 2023;2597:105–20. doi:10.1007/978-1-0716-2835-5.
22. Kumar P, Nagarajan A, Uchil PD. Analysis of cell viability by the MTT assay. Cold Spring Harb Protoc. 2018;2018(6):pdb.prot095505. doi:10.1101/pdb.prot095505.
23. Schmittgen TD, Zakrajsek BA. Effect of experimental treatment on housekeeping gene expression: validation by real-time, quantitative RT-PCR. J Biochem Biophys Methods. 2000;46(1–2):69–81. doi:10.1016/S0165-022X(00)00129-9.
24. Eruslanov E, Kusmartsev S. Identification of ROS using oxidized DCFDA and flow-cytometry. Methods Mol Biol. 2010;594:57–72. doi:10.1007/978-1-60761-411-1.
25. Choi HS, Kim JW, Cha YN, Kim C. A quantitative nitroblue tetrazolium assay for determining intracellular superoxide anion production in phagocytic cells. J Immunoassay Immunochem. 2006;27(1):31–44. doi:10.1080/15321810500403722.
26. Vermes I, Haanen C, Steffens-Nakken H, Reutelingsperger C. A novel assay for apoptosis. Flow cytometric detection of phosphatidylserine expression on early apoptotic cells using fluorescein labelled Annexin V. J Immunol Methods. 1995;184(1):39–51. doi:10.1016/0022-1759(95)00072-I.
27. Bloise FF, Oliveira FL, Nobrega AF, Vasconcellos R, Cordeiro A, Paiva LS, et al. High levels of circulating triiodothyronine induce plasma cell differentiation. J Endocrinol. 2014;220(3):305–17. doi:10.1530/JOE-13-0315.
28. Robinson MV, Obut TA, Melnikova EV, Trufakin VA. Parameters of cellular and humoral immunity in experimental hyperthyroidism and its correction. Bull Exp Biol Med. 2014;156(4):473–5. doi:10.1007/s10517-014-2377-4.
29. Hoffmann JP, Liu JA, Seddu K, Klein SL. Sex hormone signaling and regulation of immune function. Immunity. 2023;56(11):2472–91. doi:10.1016/j.immuni.2023.10.008.
30. Dunn SE, Perry WA, Klein SL. Mechanisms and consequences of sex differences in immune responses. Nat Rev Nephrol. 2024;20(1):37–55. doi:10.1038/s41581-023-00787-w.
31. Ortona E, Pierdominici M, Rider V. Editorial: sex hormones and gender differences in immune responses. Front Immunol. 2019;10:1076. doi:10.3389/fimmu.2019.01076.
32. Xu H, Liew LN, Kuo IC, Huang CH, Goh DL, Chua KY. The modulatory effects of lipopolysaccharide-stimulated B cells on differential T-cell polarization. Immunology. 2008;125(2):218–28. doi:10.1111/j.1365-2567.2008.02832.x.
33. Burger C, Vitetta ES. The response of B cells in spleen, Peyer's patches, and lymph nodes to LPS and IL-4. Cell Immunol. 1991;138(1):35–43. doi:10.1016/0008-8749(91)90130-4.
34. Rubingh J, van der Spek A, Fliers E, Boelen A. The role of thyroid hormone in the innate and adaptive immune response during infection. Compr Physiol. 2020;10(4):1277–87. doi:10.1002/cphy.c200003.
35. Chatterjee S, Chandel AS. Immunomodulatory role of thyroid hormones: *in vivo* effect of thyroid hormones on the blastogenic response of lymphoid tissues. Acta Endocrinol. 1983;103(1):95–100. doi:10.1530/acta.0.1030095.

36. Marín-García J. Thyroid hormone and myocardial mitochondrial biogenesis. Vascul Pharmacol. 2010;52(3–4): 120–30. doi:10.1016/j.vph.2009.10.008.
37. Cioffi F, Senese R, Lanni A, Goglia F. Thyroid hormones and mitochondria: with a brief look at derivatives and analogues. Mol Cell Endocrinol. 2013;379(1–2):51–61. doi:10.1016/j.mce.2013.06.006.
38. Al-Suhaimi E, AlQuwaie R, AlSaqabi R, Winarni D, Dewi FRP, AlRubaish AA, et al. Hormonal orchestra: mastering mitochondria's role in health and disease. Endocrine. 2024;86(3):903–29. doi:10.1007/s12020-024-03967-1.
39. Venediktova N, Solomadin I, Nikiforova A, Starinets V, Mironova G. Functional state of rat heart mitochondria in experimental hyperthyroidism. Int J Mol Sci. 2021;22(21):11744. doi:10.3390/ijms222111744.
40. Venediktova N, Solomadin I, Starinets V, Mironova G. Structural and dynamic features of liver mitochondria and mitophagy in rats with hyperthyroidism. Int J Mol Sci. 2022;23(22):14327. doi:10.3390/ijms232214327.
41. Venditti P, Napolitano G, Di Meo S. Role of mitochondria and other ROS sources in hyperthyroidism-linked oxidative stress. Immunol Endocr Metab Agents Med Chem. 2015;15(1):5–36. doi:10.2174/1871522215011507101249 51.
42. Barreiro Arcos ML. Role of thyroid hormones-induced oxidative stress on cardiovascular physiology. Biochim Biophys Acta Gen Subj. 2022;1866(12):130239. doi:10.1016/j.bbagen.2022.130239.
43. Costilla M, Macri Delbono R, Klecha A, Cremaschi GA, Barreiro Arcos ML. Oxidative stress produced by hyperthyroidism status induces the antioxidant enzyme transcription through the activation of the nrf-2 factor in lymphoid tissues of balb/c mice. Oxid Med Cell Longev. 2019;2019:7471890. doi:10.1155/2019/7471890.
44. Pecchillo Cimmino T, Ammendola R, Cattaneo F, Esposito G. NOX dependent ROS generation and cell metabolism. Int J Mol Sci. 2023;24(3):2086. doi:10.3390/ijms24032086.
45. Bortolotti M, Polito L, Battelli MG, Bolognesi A. Xanthine oxidoreductase: one enzyme for multiple physiological tasks. Redox Biol. 2021;41:101882. doi:10.1016/j.redox.2021.101882.
46. Saban M, Costilla M, Klecha AJ, Di Cugno M, Curria MI, Cremaschi G, et al. Regulation of the cellular redox state and the expression of DNA methyltransferase-1 in peripheral blood mononuclear cells from patients with Graves' disease. Endocrinol Diabetes Nutr. 2022;69(6):409–17. doi:10.1016/j.endinu.2021.07.011.
47. Lin HY, Glinsky GV, Mousa SA, Davis PJ. Thyroid hormone and anti-apoptosis in tumor cells. Oncotarget. 2015;6(17):14735–43. doi:10.18632/oncotarget.4023.
48. Ning Y, Jia Y, Yang Y, Wen W, Huang M, Liu S, et al. Thyroid hormones inhibit apoptosis of macrophage induced by oxidized low-density lipoprotein. Biofactors. 2022;48(1):86–99. doi:10.1002/biof.1803.
49. Liu YC, Yeh CT, Lin KH. Molecular functions of thyroid hormone signaling in regulation of cancer progression and anti-apoptosis. Int J Mol Sci. 2019;20(20):4986. doi:10.3390/ijms20204986.
50. Di Meo S, Venditti P. Evolution of the knowledge of free radicals and other oxidants. Oxid Med Cell Longev. 2020;2020:9829176. doi:10.1155/2020/9829176.